

Article

# Successful Release of Voriconazole and Flavonoids from MAPLE Deposited Bioactive Surfaces

Irina Negut <sup>1,2</sup>, Anita Ioana Visan <sup>1</sup>, Camelia Popescu <sup>1</sup>, Rodica Cristescu <sup>1,\*</sup>, Anton Fikai <sup>3</sup>, Alexandru Mihai Grumezescu <sup>3</sup>, Mariana C. Chifiriuc <sup>4</sup>, Ryan D. Boehm <sup>5</sup>, Dina Yamaleyeva <sup>5</sup>, Michael Taylor <sup>5</sup>, Roger J. Narayan <sup>5,\*</sup> and Douglas B. Chrisey <sup>6</sup>

<sup>1</sup> Lasers Department, National Institute for Lasers, Plasma & Radiation Physics, P.O. Box MG-36, 077125 Bucharest-Magurele, Romania; negut.irina@inflpr.ro (I.N.); anita.visan@inflpr.ro (A.V.); camelia.popescu@inflpr.ro (C.P.)

<sup>2</sup> Faculty of Physics, University of Bucharest, 050107 Bucharest, Romania

<sup>3</sup> Faculty of Applied Chemistry and Materials Science, Politehnica University of Bucharest, 1–7 Polizu Street, 011061 Bucharest, Romania; anton.fikai@upb.ro (A.F.); grumezescu@yahoo.com (A.M.G.)

<sup>4</sup> Microbiology Immunology Department, Faculty of Biology and Research Institute of the University of Bucharest (ICUB), University of Bucharest, 77206 Bucharest, Romania; carmen\_balotescu@yahoo.com

<sup>5</sup> Department of Biomedical Engineering, University of North Carolina, Chapel Hill, NC 27599, USA; ryandboehm@gmail.com (R.D.B.); dnyamale@ncsu.edu (D.Y.); matayl10@ncsu.edu (M.T.)

<sup>6</sup> Department of Physics and Engineering Physics, Tulane University, New Orleans, LA 70118, USA; dchrisey@tulane.edu

\* Correspondence: rodica.cristescu@inflpr.ro (R.C.); roger\_narayan@unc.edu (R.J.N.); Tel.: +40-(0)21-457-4550 (R.C.); +1-919-696-8488 (R.J.N.)

Received: 17 January 2019; Accepted: 15 February 2019; Published: 22 February 2019



**Featured Application:** Biomimetic thin films deposited by matrix-assisted pulsed laser evaporation (MAPLE) have a promising potential for use in designing medical device surfaces with antifungal activity for releasing combinations of natural flavonoids (quercetin dihydrate and resveratrol) and antifungal compounds (amphotericin B and voriconazole) embedded in a polyvinylpyrrolidone biopolymer. MAPLE may offer a viable alternative for antimicrobial coating synthesis with specific advantages in implant fabrication.

**Abstract:** We explored the potential of biomimetic thin films fabricated by means of matrix-assisted pulsed laser evaporation (MAPLE) for releasing combinations of active substances represented by flavonoids (quercetin dihydrate and resveratrol) and antifungal compounds (amphotericin B and voriconazole) embedded in a polyvinylpyrrolidone biopolymer; the antifungal activity of the film components was evaluated using *in vitro* microbiological assays. Thin films were deposited using a pulsed KrF\* excimer laser source which were structurally characterized using atomic force microscopy (AFM) and Fourier transform infrared spectroscopy (FTIR). High-quality thin films with chemical structures similar to dropcast ones were created using an optimum laser fluence of ~80 mJ/cm<sup>2</sup>. Bioactive substances were included within the polymer thin films using the MAPLE technique. The results of the *in vitro* microbiology assay, which utilized a modified disk diffusion approach and were performed using two fungal strains (*Candida albicans* American Type Culture Collection (ATCC) 90028 and *Candida parapsilosis* American Type Culture Collection (ATCC) 22019), revealed that voriconazole was released in an active form from the polyvinylpyrrolidone matrix. The results of this study show that the MAPLE-deposited bioactive thin films have a promising potential for use in designing combination products and devices, such as drug delivery devices, and medical device surfaces with antifungal activity.

**Keywords:** flavonoid; quercetin dihydrate; resveratrol; biopolymer; matrix-assisted pulsed laser evaporation; antifungal activity

## 1. Introduction

*Candida* species are emerging as a major cause of nosocomial infections. Sessile *Candida* cells exhibit a high resistance to antifungal agents depending on their biochemical, genetic and/or morphological flexibility that enables adaptation to an extensive range of host defense mechanisms. Moreover, the pathogenic activity of *Candida* spp. is primarily attributed to their high capability to form biofilms on the surfaces of medical devices [1]. Medical device-associated *Candida* spp. biofilms are refractory to many conventional therapies and can lead to significant complications. Furthermore, *Candida* spp. infections are more likely to occur and progress more severely in immunosuppressed patients [2].

The most frequently used types of antifungal agents against *Candida* spp. infections include azoles, polyenes, pyrimidine analogs, and echinocandins [3]. From polyene agents, amphotericin B displays the broadest spectrum and most effective fungicidal activity. Even though amphotericin B is usually preferred among antifungal agents, its use at high doses over an extended time period is associated with side effects such as anemia, hypertension, tremors, and even renal failure [4]. Voriconazole is a new second-generation triazole antifungal agent with a broad-spectrum of activity against opportunistic fungal pathogens, including *Candida* spp. and *Aspergillus* spp. [5]. On the other hand, the pharmacokinetic behavior of this triazole is non-linear and presents a narrow therapeutic window, resulting in under-dosage and/or dose-dependent adverse effects [6].

The management of medical device-*Candida* spp. contaminations faces numerous problems, such as toxicity caused by prolonged treatment with high doses, resistance to conventional therapy, recurrence of infection, and the high treatment costs [7]. In addition, the removal/replacement of an infected medical device may be a challenging because of the patient state and condition [8]. In order to preserve implanted devices, it is therefore imperative to develop new and effective therapeutic strategies for the treatment of *Candida* spp. biofilms and associated infections, such as associations of two or more antifungals [9], alternative agents (e.g., natural products) or a combination of antifungals and natural compounds [10], as well as more efficient drug delivery systems [11,12].

Many compounds, extracts, and derivatives of plant origin have been found to be effective and safe antifungal agents, and have a much more acceptable toxicity as compared to commonly used antifungals. Among plant-derived bioactive substances, phenolic plant compounds such as resveratrol and quercetin flavonoids have been shown to inhibit the growth of different pathogenic microorganisms, including fungi [13,14].

Polymeric thin films have been intensively studied for use in novel drug delivery systems due to their intrinsic properties (e.g., tunable size, form, solubility, stability and degradability, high surface/volume ratio, versatile and easy functionalization, biocompatibility, and biomimetic properties) [15]. Polymeric thin films can be deposited on medical devices by a variety of techniques [16]—matrix-assisted pulsed laser evaporation (MAPLE) [17] has been shown to produce continuous coatings containing various drugs with a high encapsulation efficiency [18].

A core drug is commonly encapsulated within a thin layer of the coating material (e.g., a biodegradable polymer). The coating may be modified in various ways to slow the release rate of the active biomaterial or increase the absorption of the drug into the systemic circulation. The MAPLE approach offers several benefits over conventional encapsulation techniques, including: (a) it is a rapid process that can be completed in several minutes; (b) it is compatible with a variety of materials, enabling thin films to be produced from materials with known biocompatibility properties; (c) it is a dry technique that can be performed using sterile methods; and (d) drug agglomeration can possibly be minimized. Depositing coatings over drugs may facilitate the control of drug release kinetics by: (a) adjusting the drug diffusion through the coating, or (b) coating degradation which enables the drug release [19–23].

In our previous work, we used the MAPLE technique as a new approach for the deposition of coatings containing gentamicin [24,25] embedded polymeric matrices or silver nanoparticles for antimicrobial applications [26]. In view of obtaining improved coatings capable of modulating and controlling microbial biofilm behavior, we used MAPLE to fabricate thin films resistant to microbial colonization, containing natural (quercetin flavonoid) and synthetic (norfloxacin and cefuroxime antibiotics) compounds. Quercetin-containing coatings showed better resistance to microbial colonization than antibiotic-containing ones [27].

In the present study, we used MAPLE to prepare different biomimetic thin films containing the polyvinylpyrrolidone biopolymer: polyvinylpyrrolidone–antibiotic, polyvinylpyrrolidone–flavonoid, and polyvinylpyrrolidone–flavonoid–antibiotic thin films. The chemical structures and morphologies of thin films were examined. The antifungal activity of the thin films against two yeast strains was investigated to assess the potential of these materials for the development of novel antimicrobial strategies.

## 2. Materials and Methods

### 2.1. Materials

Flavonoids (quercetin dihydrate and resveratrol), antimicrobial agents (amphotericin B and voriconazole), biopolymer (polyvinylpyrrolidone), and dimethyl sulfoxide (DMSO) solvent used in MAPLE target preparation were obtained from commercial sources. Quercetin dihydrate was obtained from Sigma-Aldrich, St. Louis, MO, USA. Resveratrol was obtained from Sigma-Aldrich Chemie GmbH, Steinheim, Germany. Both amphotericin B and voriconazole were obtained from Fisher Scientific, Fair Lawn, New Jersey, USA.

Microbial cultures (*C. albicans*, American Type Culture Collection (ATCC) 90028 and *C. parapsilosis*, American Type Culture Collection (ATCC) 22019) were acquired from American Type Culture Collection, Manassas, VA. Microbial culture materials were acquired from BD Diagnostics, Franklin Lakes, NJ. The yeast mold (YM) broth, Mueller-Hinton agar media, and Sabouraud's dextrose agar media were obtained from Teknova, Hollister, CA, USA.

### 2.2. MAPLE Experimental Conditions

Solutions comprising dimethyl sulfoxide and combinations of polyvinylpyrrolidone, flavonoids (quercetin dihydrate or resveratrol), and/or antimicrobial agents (amphotericin B or voriconazole) were prepared at room temperature: polyvinylpyrrolidone; 10:1 polyvinylpyrrolidone:flavonoid, 10:1 polyvinylpyrrolidone:antibiotic, or 10:1:1 polyvinylpyrrolidone:flavonoid:antibiotic. It should be noted that all of the solutions contained 2 wt% polyvinylpyrrolidone in DMSO.

Before each deposition, 3.5 mL of the newly prepared solution was placed using a syringe in a pre-cooled copper target holder that had a 3 cm diameter and a 5 mm height. The MAPLE cryogenic target was created by placing the target in a Dewar vessel, which contained liquid nitrogen. After the freezing step, the target holder was quickly placed in the target position within the MAPLE chamber. The MAPLE thin films were deposited onto optical glass substrates and one-side-polished Si <100> wafers. In order to get clean and sterilized substrates, we used both an ethanol ultrasonic bath and a UV lamp (VL115-Vilber Lourmat Deutschland GmbH, Eberhardzell, Germany). A KrF\* excimer laser source ( $\lambda = 248 \text{ nm}$ @10 Hz, 25 ns pulse duration, model COMPexPro 205 (Lambda Physics-Coherent, Göttingen, Germany)) was utilized for MAPLE deposition. The laser beam browsed the target surface at a 45° angle. A laser beam homogenizer was utilized to enhance the distribution of energy for the laser spot and increase the coated region on the substrate. For each deposition, we used the following parameters: 300 mJ laser energy, 36 mm<sup>2</sup> beam spot area, and 100,000 subsequent laser pulses. During MAPLE experiments, the target and substrate were placed at 5 cm separation distance. Both were rotated at a rate of 0.4 Hz. The rotating target was kept in direct contact with a cooling device that contained a liquid nitrogen reservoir connected to the target using copper pipes.

### 2.3. Characterization Methods

#### 2.3.1. Fourier-Transform Infrared Spectroscopy (FTIR) Investigations

The structural characterization of obtained MAPLE thin films and corresponding starting materials (dropcast) were performed using a Nicolet iN10 MX FTIR microscope (Thermo Fisher Scientific, Waltham, MA, USA) with a mercury cadmium telluride (MCT) liquid nitrogen-cooled detector, performed in reflection mode ( $4\text{ cm}^{-1}$  resolution), within the range of  $4000\text{--}600\text{ cm}^{-1}$ . The registered scans were co-added and transferred to absorbance values using OmnicPicta software (Thermo Scientific, Waltham, MA, USA). IR spectra maps displayed the spectral absorbance of characteristic wavenumbers in color changes starting with blue color (the lowest intensity) and increasing through green, yellow, and red colors (the highest intensity).

#### 2.3.2. Atomic Force Microscope (AFM) Studies

The morphology of MAPLE thin films was recorded with an optical beam bounce scanning probe microscope, Dimension 3000 (Bruker AFM Probes, Camarillo, CA, USA), which was equipped with NanoScope analysis software. Scans of  $10 \times 10\ \mu\text{m}^2$  regions of individual thin films were collected in contact mode.

#### 2.3.3. Microbial Strains Used for Antifungal Activity Assay

The antifungal activity of the samples was examined using a modified agar diffusion assay with two fungal strains (*C. albicans*, ATCC 90028 and *C. parapsilosis*, ATCC 22019).

Freeze-dried ampoules were rehydrated with distilled water and a few droplets were added to culture tubes of YM broth. These broth cultures were incubated overnight at  $30\text{ }^\circ\text{C}$  and  $5\%$   $\text{CO}_2$ . After incubation of these fungal strains, the broth cultures were centrifuged at  $4500\text{ rpm}$  for  $10\text{ minutes}$ . The cell pellets were re-suspended in  $1\times\text{ PBS}$  (phosphate-buffered saline) to obtain an optical density of  $0.5$  McFarland turbidity standard. The suspensions of *C. albicans* were used to inoculate lawns of fungi onto plates of modified Mueller-Hinton agar using cotton-tipped applicator swabs. The Mueller-Hinton agar plates had been altered by the addition of  $1.5\text{ mL}$  of a solution containing  $2\%$  glucose and  $0.5\ \mu\text{g/mL}$  methylene blue. Similarly, lawns of *C. parapsilosis* were inoculated onto Sabouraud's dextrose agar plates.

Positive controls consisted of glass cover slips ( $22 \times 22\text{ mm}^2$ ) that were treated with a  $1\ \mu\text{g}$  dose of voriconazole (in DMSO). A  $4\ \mu\text{L}$  droplet of voriconazole in DMSO was applied to the surface of the glass cover slips. The negative controls for this study were untreated cover slips with the same dimensions as the positive controls. Each test sample and control were plated onto the fungal lawns shortly following inoculation. The samples were incubated overnight at  $35\text{ }^\circ\text{C}$  (*C. albicans*) or  $30\text{ }^\circ\text{C}$  (*C. parapsilosis*) with  $5\%$   $\text{CO}_2$ . The plates that contained the test samples and controls were evaluated after  $24\text{ hours}$  for areas of inhibited growth and imaged using a digital camera and a dissection microscope ( $8\times$  magnification).

#### 2.3.4. Statistical Analysis

The results were statistically analyzed using the two-way analysis of variance (ANOVA) test (Bonferroni post-test) with Graph Pad Prism v5 software, GraphPad Software, La Jolla, CA, USA, [www.graphpad.com](http://www.graphpad.com) ( $p$ -values lower than  $0.05$  were considered to be significant).

## 3. Results

### 3.1. FTIR Investigations

IR maps of dropcast and MAPLE thin films are presented in Figure 1. Surface mapping exhibited the chemical properties and the distribution of functional groups across the sample region.

The mapping intensities were recorded based on the IR absorbance intensity values of the examined peaks [28]. Typical FTIR spectra of the MAPLE-deposited samples are shown in Figure 2.

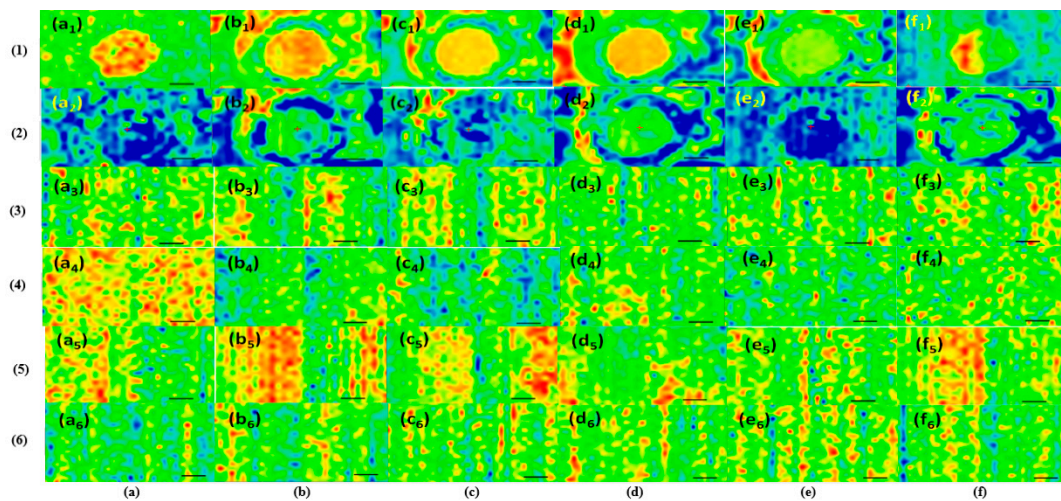


**Figure 1.** Infrared spectroscopy (IR) mapping data. Intensity distribution of dropcast surfaces: (1) polyvinylpyrrolidone–quercetin dihydrate–amphotericin B and (2) polyvinylpyrrolidone–resveratrol–voriconazole. Intensity distribution of thin films deposited by matrix-assisted pulsed laser evaporation (MAPLE): (3) polyvinylpyrrolidone–quercetin dihydrate–amphotericin B, (4) polyvinylpyrrolidone–resveratrol–amphotericin B, (5) polyvinylpyrrolidone–quercetin dihydrate–voriconazole, and (6) polyvinylpyrrolidone–resveratrol–voriconazole, where monitored peaks: ( $a_1$ – $a_6$ ):  $2957\text{ cm}^{-1}$ ; ( $b_1$ – $b_6$ ):  $1672\text{ cm}^{-1}$ ; ( $c_1$ – $c_6$ ):  $1461\text{ cm}^{-1}$ ; ( $d_1$ – $d_6$ ):  $1291\text{ cm}^{-1}$ ; ( $e_1$  and  $e_3$ ):  $1620\text{ cm}^{-1}$ ; ( $f_1$  and  $f_3$ ):  $3310\text{ cm}^{-1}$ ; ( $e_2, e_4, e_5$ , and  $e_6$ ):  $1270\text{ cm}^{-1}$ ; ( $f_2, f_4, f_5$ , and  $f_6$ ):  $1644\text{ cm}^{-1}$ .

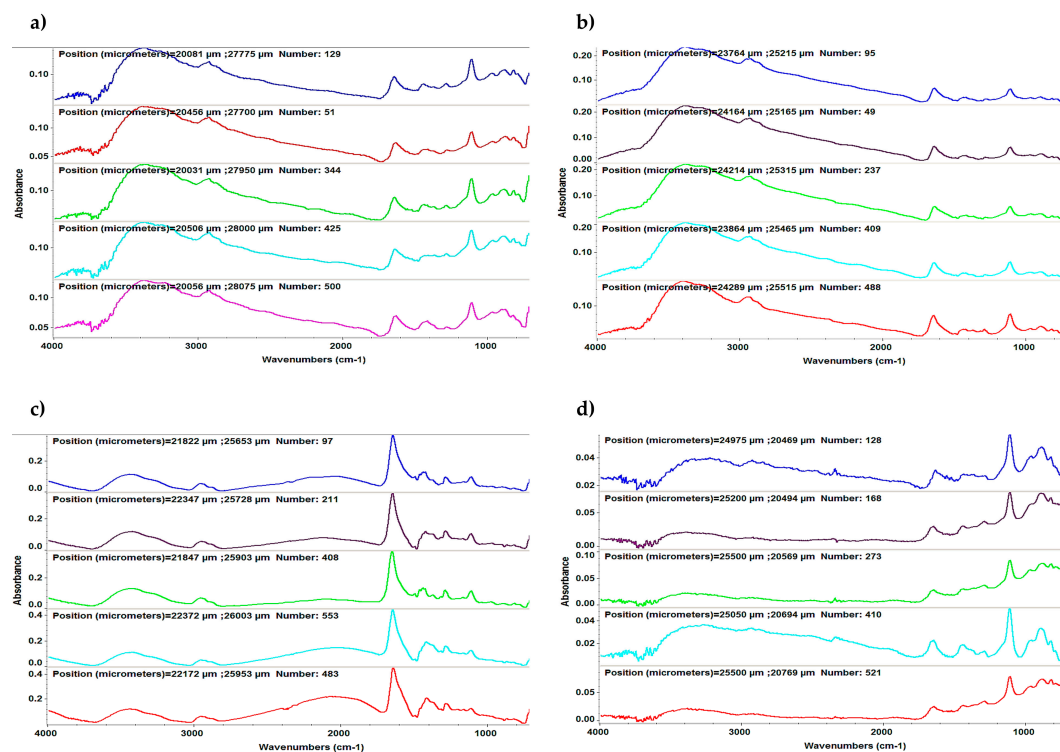


**Figure 2.** Typical Fourier-transform infrared spectroscopy (FTIR) spectra of MAPLE-deposited thin films: (a) polyvinylpyrrolidone–quercetin dihydrate–amphotericin B, (b) polyvinylpyrrolidone–resveratrol–amphotericin B, (c) polyvinylpyrrolidone–quercetin dihydrate–voriconazole, and (d) polyvinylpyrrolidone–resveratrol–voriconazole.

### 3.2. AFM Studies

Three-dimensional topographical images showing the surface morphologies of the MAPLE-deposited coatings are provided in Figure 3. The root mean square (RMS) roughness values and Z-range values for the  $10 \times 10 \mu\text{m}^2$  scans of the thin films are also indicated in Figure 3 and Table 1.

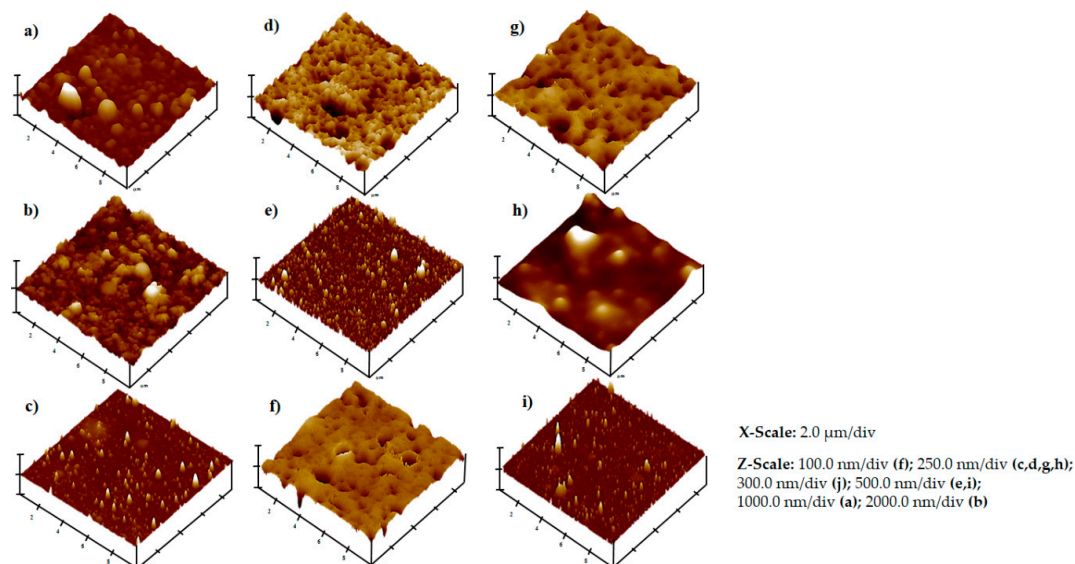


**Figure 3.** Surface data for MAPLE-deposited thin films, including  $10 \times 10 \mu\text{m}^2$  atomic force microscope (AFM) scans, root mean square (RMS) roughness, and Z-range values: (a) polyvinylpyrrolidone, (b) polyvinylpyrrolidone–quercetin dihydrate, (c) polyvinylpyrrolidone–quercetin dihydrate–amphotericin B, (d) polyvinylpyrrolidone–quercetin dihydrate–voriconazole, (e) polyvinylpyrrolidone–resveratrol–voriconazole, (f) polyvinylpyrrolidone–resveratrol–amphotericin B, (g) polyvinylpyrrolidone–resveratrol, (h) polyvinylpyrrolidone–voriconazole, and (i) polyvinylpyrrolidone–amphotericin B.

**Table 1.** Atomic force microscope (AFM) surface roughness analysis of thin film surfaces.

Roughness Parameter Values	(a)	(b)	(c)	(d)	(e)	(f)	(g)	(h)	(i)
Root mean square (RMS) (nm)	117.6	169.2	10.5	21.4	32.4	15.7	19.7	46.5	15.4
Z-Range ( $\mu\text{m}$ )	1.59	1.45	0.163	0.170	0.357	0.230	0.199	0.360	0.327

### 3.3. Antifungal Activity

A modification of the disk diffusion assay was used to examine fungal cultures that were incubated in contact with the MAPLE-deposited thin films. Zones of growth inhibition in the fungal cultures were indicative of the antifungal activity of the tested materials and the diameters of the zones were measured to the nearest millimeter. Images of the evaluated samples are provided in Figures 4 and 5, and the values of the diameters of the growth inhibition zones are shown in Figure 6.

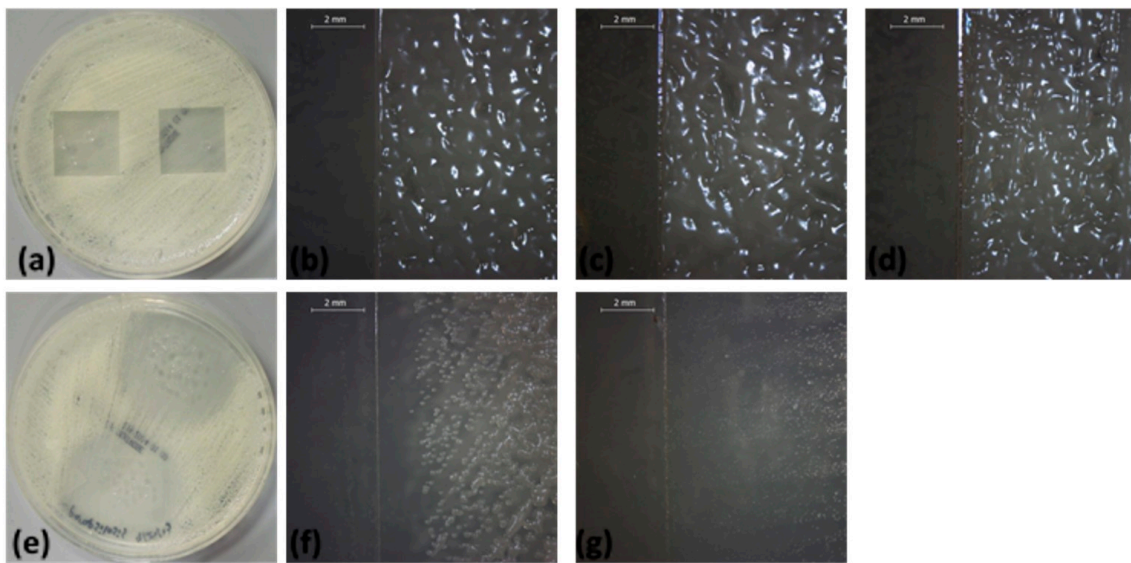


**Figure 4.** Modified disk diffusion images of samples plated with *C. parapsilosis*: (a) macroscopic plate view of negative control, (b) negative control, (c) polyvinylpyrrolidone, (d) polyvinylpyrrolidone–amphotericin B, (e) macroscopic plate view of positive control, (f) positive control, and (g) polyvinylpyrrolidone–voriconazole.

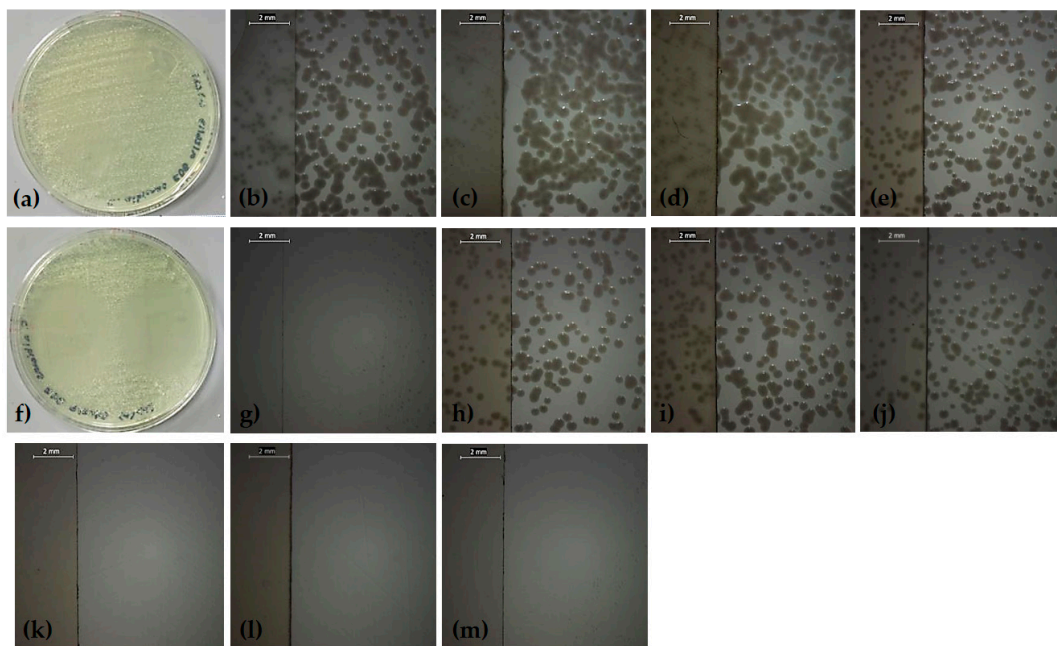


**Figure 5.** Modified disk diffusion images of samples plated with *C. albicans*: (a) macroscopic view of negative control, (b) negative control, (c) polyvinylpyrrolidone, (d) polyvinylpyrrolidone–quercetin dihydrate, (e) polyvinylpyrrolidone–resveratrol, (f) macroscopic view of positive control, (g) positive control, (h) polyvinylpyrrolidone–quercetin dihydrate–amphotericin B, (i) polyvinylpyrrolidone–resveratrol–amphotericin B, (j) polyvinylpyrrolidone–amphotericin B, (k) polyvinylpyrrolidone–voriconazole, (l) polyvinylpyrrolidone–quercetin dihydrate–voriconazole, and (m) polyvinylpyrrolidone–resveratrol–voriconazole.

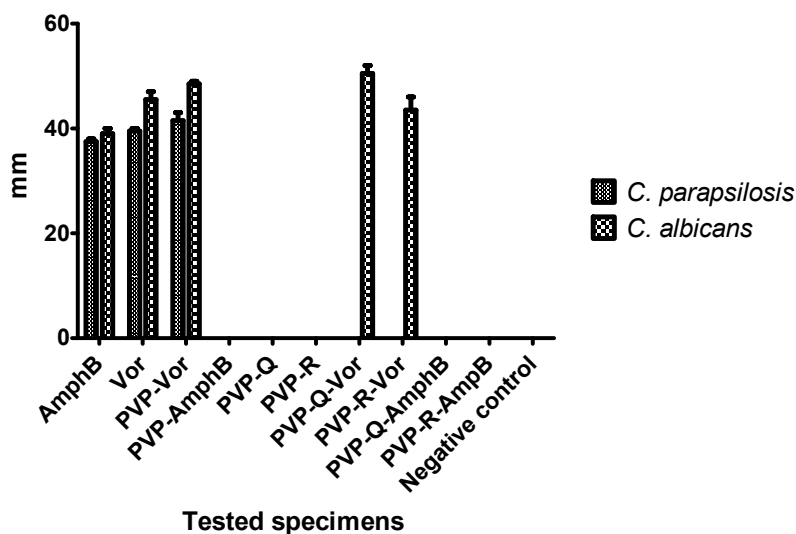


**Figure 6.** Graphic representation of fungal growth inhibition diameters obtained in the presence of different thin films. Positive controls—amphotericin B (AmphB), voriconazole (Vor), polyvinylpyrrolidone–voriconazole (PVP-Vor), polyvinylpyrrolidone–amphotericin B (PVP-AmphB), polyvinylpyrrolidone–quercetin dehydrate (PVP-Q), polyvinylpyrrolidone–resveratrol (PVP-R), polyvinylpyrrolidone–resveratrol–voriconazole (PVP-Q-Vor), polyvinylpyrrolidone–quercetin dihydrate–amphotericin B (PVP-R-Vor), polyvinylpyrrolidone–quercetin dihydrate–amphotericin B (PVP-Q-AmphB), and polyvinylpyrrolidone–resveratrol–amphotericin B (PVP-R-AmphB); Negative control—sterile microscopic slides.

#### 4. Discussion

Four IR absorption features characteristic of polyvinylpyrrolidone macromolecule were selected as spectral markers for polyvinylpyrrolidone in the thin films (Figure 1). These selected IR absorption features were as follows:  $2957\text{ cm}^{-1}$  (characteristic C-H stretching vibrations) visible in Figure 1 a<sub>1</sub>–a<sub>6</sub>;  $1672\text{ cm}^{-1}$  (the vibration band of the C=O group) evidenced in Figure 1 b<sub>1</sub>–b<sub>6</sub>;  $1461\text{ cm}^{-1}$  (bending vibration of the CH<sub>2</sub> group) shown in Figure 1 c<sub>1</sub>–c<sub>6</sub>, and  $1291\text{ cm}^{-1}$  (the C–N stretching vibration of N-vinyl pyrrolidone) presented in Figure 1 d<sub>1</sub>–d<sub>6</sub>. Two absorption bands known as being characteristic of amphotericin B were selected as spectral markers:  $1620\text{ cm}^{-1}$  (symmetric stretching vibrations of the hydrogen-bonded C=O group in the non-ionized carboxyl group) exhibited in Figure 1 e<sub>1</sub> and e<sub>3</sub>, and  $3310\text{ cm}^{-1}$  (assigned to the C–N stretching vibrations in the NH<sub>2</sub> group) revealed in Figure 1 f<sub>1</sub> and f<sub>3</sub>. The absorption band noted in quercetin dihydrate was selected as a spectral marker— $1100\text{ cm}^{-1}$  (C–OH stretching vibration)—while the characteristic absorption band of resveratrol was selected as a spectral marker— $3400\text{ cm}^{-1}$  (OH group) [26]. Two absorption bands known as being characteristic of voriconazole were selected as a spectral marker— $1270\text{ cm}^{-1}$  (C–F vibration) displayed in Figure 1 e<sub>2</sub>, e<sub>4</sub>, e<sub>5</sub>, and e<sub>6</sub>, and  $1644\text{ cm}^{-1}$  (C=N) as exposed in Figure 1 f<sub>2</sub>, f<sub>4</sub>, f<sub>5</sub>, and f<sub>6</sub>. The observed differences in the FTIR spectra are due to different absorption bands specific to each composite configuration: polyvinylpyrrolidone–quercetin dihydrate–amphotericin B (Figure 2a), polyvinylpyrrolidone–resveratrol–amphotericin B (Figure 2b), polyvinylpyrrolidone–quercetin dihydrate–voriconazole (Figure 2c), and polyvinylpyrrolidone–resveratrol–voriconazole (Figure 2d). FTIR spectra revealed that MAPLE is suitable for preparing polyvinylpyrrolidone–flavonoid–antibiotic composite thin films with chemical structures close to those of the starting materials.

Important information was also acquired by AFM analyses. No grain boundaries and a lack of large material agglomerates were observed in the scanned samples. The scans of polyvinylpyrrolidone with quercetin dehydrate, as well as polyvinylpyrrolidone, only showed the highest roughness values ( $> 100\text{ nm}$ ) and z-ranges ( $> 1.4\text{ }\mu\text{m}$ ) among the scanned materials. The thin films that contained resveratrol or amphotericin B showed surface roughness values at the lower end among the scanned

samples (Figure 3). The polyvinylpyrrolidone–quercetin dehydrate–amphotericin B sample had the lowest surface roughness and z-range values among all of the scanned samples (Table 1).

In the current study, the ability of our biomimetic coatings to inhibit the development of biofilms formed by *C. parapsilosis* and *C. albicans*, two organisms which are frequently medical device-associated infections, was determined under *in vitro* conditions. The obtained results were significantly different for the two strains ( $p < 0.001$ ). For *C. parapsilosis* (Figures 4 and 6), zones of growth inhibition were observed for the positive controls (voriconazole and amphotericin B) and for polyvinylpyrrolidone–voriconazole samples. The occurrence of growth inhibition zones indicates that these materials have antifungal activity against *C. parapsilosis*, resulting in a lack of observable colony forming units in the regions surrounding the samples. This observation suggests that the antifungal activity of the respective samples is not limited to a surface interaction between the thin films and the fungal cells. The anti-biofilm activity of the coatings tested against *C. albicans* biofilms are shown in Figure 5. The growth inhibition zones surrounding the samples were noted for the positive controls, the polyvinylpyrrolidone–voriconazole samples, the polyvinylpyrrolidone–quercetin dihydrate–voriconazole samples, and the polyvinylpyrrolidone–resveratrol–voriconazole samples (Figure 6).

The analysis of the coating efficiency against *C. albicans* versus *C. parapsilosis* biofilms indicated a statistically significant higher activity of voriconazole, polyvinylpyrrolidone–voriconazole, polyvinylpyrrolidone–quercetin dihydrate–voriconazole, and polyvinylpyrrolidone–resveratrol–voriconazole samples against *C. albicans* biofilms as compared with *C. parapsilosis* (two-way ANOVA, Bonferroni post-test,  $p < 0.001$ ). The coating containing voriconazole embedded in polyvinylpyrrolidone and polyvinylpyrrolidone–quercetin dihydrate–voriconazole proved to be significantly more active than free voriconazole against *C. albicans* biofilms ( $p < 0.05$  and  $p < 0.0001$ , respectively). The coatings containing both voriconazole and quercetin dehydrate exhibited higher activity against *C. albicans* biofilms as compared with the coatings containing either voriconazole or quercetin dehydrate alone ( $p < 0.001$ ). In the case of *C. parapsilosis* biofilms, the coatings containing polyvinylpyrrolidone–voriconazole proved to be more active than free voriconazole ( $p < 0.001$ ). Our results are in agreement with other scientific reports, which demonstrates the synergy between polyvinylpyrrolidone or quercetin and azoles. For example, it was shown that quercetin combined with fluconazole exhibited synergistic activity against the *C. albicans* biofilm formed by strains isolated from patients with vulvovaginal candidiasis due to the inhibition of cell–cell adhesion and the expression of genes responsible for biofilm formation (e.g., *ALS1*, *HWP1*, *SUN41*, *UME6*, *PBS2*, and *PDE2*) [29].

Polyvinylpyrrolidone polymer is used as a granulation binder excipient for voriconazole tablets [30]. Other recent studies demonstrated synergy between polyvinylpyrrolidone-coated silver nanoparticles (Ag-NPs) and azole antifungals (e.g., voriconazole) against a drug-resistant *C. albicans* strain. Several changes were detected after the combination treatment, including disruption of cell membrane integrity, the tendency of polyvinylpyrrolidone-coated Ag-NPs to adhere to the cell membrane, inhibition of the budding process, as well as defects in ergosterol signaling and efflux pump functions [31].

The synergic antifungal activity of polyvinylpyrrolidone, quercetin, and voriconazole may be explained by better interaction of fluconazole with the fungal cells and/or biofilm matrix, the inhibition of intercellular communication and adhesion, changes in gene expression profile, alteration of membrane permeability, and interference with cellular wall synthesis.

The lack of observable colony forming units in the zones surrounding these samples is indicative of an antifungal effect that is not limited to contact between the thin films and the organisms. However, although no zones of growth inhibition in the regions surrounding the samples were recorded in the case of the other tested samples, the fungal growth was completely inhibited in the area located below the tested specimen. The negative controls did not induce any fungal growth inhibition.

Taken together, these results indicate that the biopolymer polyvinylpyrrolidone represents an interesting biomimetic matrix for targeted and controlled local delivery of voriconazole, but not for the release of amphotericin B or bioactive compounds of plant origin taken separately. This drug delivery approach could maximize the therapeutic efficiency and minimize the side effects

associated with the use of voriconazole. To our knowledge, this is the first study demonstrating the antifungal activity of a MAPLE-deposited thin film in which voriconazole is released from a polyvinylpyrrolidone matrix.

## 5. Conclusions

We demonstrated that the MAPLE technique is an appropriate approach for obtaining biomimetic thin films containing combinations of the biopolymer polyvinylpyrrolidone, flavonoids (quercetin dehydrate and resveratrol), and systemic antifungal agents (amphotericin B and voriconazole) that exhibit chemical structures similar to those of the input materials. The surface features of the thin films were evaluated using AFM, which revealed no observable grain boundaries and a lack of large material agglomerates. Agar diffusion assays confirmed the antifungal activity of MAPLE-deposited films containing polyvinylpyrrolidone–voriconazole and polyvinylpyrrolidone–quercetin dihydrate–voriconazole against *C. parapsilosis* and *C. albicans*. These results indicate the potential use of polyvinylpyrrolidone polymers for developing voriconazole delivery systems that maximize the therapeutic efficiency of the antifungal agent at the infection site, as well as minimize systemic toxic effects of voriconazole. Additionally, coatings containing both voriconazole and quercetin dehydrate exhibited improved efficiency against *C. albicans* biofilms.

**Author Contributions:** The authors individual contributions are listed below: conceptualization, R.C., A.M.G., M.C.C., R.J.N., D.B.C.; methodology, I.N., A.I.V., R.C.; C.P.; software, A.M.G., M.C.C.; validation, R.C., M.C.C., R.J.N., D.B.C.; investigation, A.F., A.M.G., M.C.C., R.D.B., D.Y., M.T.; resources, R.C., R.J.N.; writing—original draft preparation, I.N.; R.C.; A.M.G., M.C.C.; writing—review and editing, R.C., M.C.C., R.J.N., D.B.C.; visualization, R.C., A.M.G., M.C.C., R.J.N., D.B.C.; supervision, R.C., M.C.C., R.J.N., D.B.C.; project administration, R.C.; funding acquisition, R.C.

**Acknowledgments:** This work was supported by a grant of Ministry of Research and Innovation, CNCS - UEFISCDI, project number PN-III-P4-ID-PCE-2016-0884, within PNCDI III.

**Conflicts of Interest:** Authors declare no conflicts of interest.

## References

1. Polke, M.; Hube, B.; Jacobsen, I.D. Candida survival strategies. *Adv. Appl. Microbiol.* **2015**, *91*, 139–235. [[CrossRef](#)] [[PubMed](#)]
2. Azzam, K.; Parvizi, J.; Jungkind, D.; Hanssen, A.; Fehring, T.; Springer, B.; Bozic, K.; Della Valle, C.; Pulido, L.; Barrack, R. Microbiological, Clinical, and Surgical Features of Fungal Prosthetic Joint Infections: A Multi-Institutional Experience. *J. Bone Jt. Surg. Am.* **2009**, *6*, 142–149. [[CrossRef](#)]
3. Carmona, E.M.; Limper, A.H. Overview of Treatment Approaches for Fungal Infections. *Clin. Chest. Med.* **2017**, *38*, 393–402. [[CrossRef](#)] [[PubMed](#)]
4. Sachan, R.; Jaipan, P.; Zhang, J.Y.; Degan, S.; Erdmann, D.; Tedesco, J.; Vanderwal, L.; Staflien, S.J.; Negut, I.; Visan, A.; et al. Printing amphotericin B on microneedles using matrix-assisted pulsed laser evaporation. *Int. J. Bioprinting* **2017**, *3*, 147–157. [[CrossRef](#)]
5. Xu, G.; Zhu, L.; Ge, T.; Liao, S.; Li, N.; Qi, F. Pharmacokinetic/pharmacodynamic analysis of voriconazole against *Candida* spp. and *Aspergillus* spp. in children, adolescents and adults by Monte Carlo simulation. *Int. J. Antimicrob. Agents* **2016**, *47*, 439–445. [[CrossRef](#)] [[PubMed](#)]
6. Mangal, N.; Hamadeh, I.S.; Arwood, M.J.; Cavallari, L.H.; Samant, T.S.; Klinker, K.P.; Bulitta, J.; Schmidt, S. Optimization of Voriconazole Therapy for the Treatment of Invasive Fungal Infections in Adults. *Clin. Pharmacol. Ther.* **2018**, *104*, 957–965. [[CrossRef](#)]
7. Martins, N.; Ferreira, I.C.; Barros, L.; Silva, S.; Henriques, M. Candidiasis: Predisposing factors, prevention, diagnosis and alternative treatment. *Mycopathologia* **2014**, *177*, 223–240. [[CrossRef](#)]
8. Pappas, P.G. Candidemia in the intensive care unit: Miles to go before we sleep. *Crit. Care Med.* **2011**, *39*, 884–885. [[CrossRef](#)]
9. Cui, J.; Ren, B.; Tong, Y.; Dai, H.; Zhang, L. Synergistic combinations of antifungals and anti-virulence agents to fight against *Candida albicans*. *Virulence* **2015**, *6*, 362–371. [[CrossRef](#)]

10. Chanda, S.; Rakholiya, K. Combination Therapy: Synergism between Natural Plant Extracts and Antibiotics against Infectious Diseases. In *Science against Microbial Pathogens: Communicating Current Research and Technological Advances (Microbiol Book Series)*; Mendez-Vilas, A., Ed.; Formatex Research Center: Badajoz, Spain, 2011; pp. 520–529.
11. Miller, R.B.; McLaren, A.C.; Pauken, C.; Clarke, H.D.; McLemore, R. Voriconazole Is Delivered From Antifungal-Loaded Bone Cement. *Clin. Orthop. Relat. Res.* **2012**, *471*, 195–200. [[CrossRef](#)]
12. Rouse, M.S.; Heijink, A.; Steckelberg, J.M.; Patel, R. Are anidulafungin or voriconazole released from polymethylmethacrylate in vitro? *Clin. Orthop. Relat. Res.* **2011**, *469*, 1466–1469. [[CrossRef](#)] [[PubMed](#)]
13. Serra, A.T.; Matias, A.A.; Nunes, A.V.M.; Leitão Brito, D.; Bronze, R.; Silva, S.; Pires, A.; Crespo, M.T.; San Romão, M.V.; Duarte, C.M. In vitro evaluation of olive- and grape-based natural extracts as potential preservatives for food. *Innov. Food Sci. Emerg. Tech.* **2008**, *9*, 311–319. [[CrossRef](#)]
14. Da Silva, C.R.; de Andrade Neto, J.B.; de Sousa Campos, R.; Figueiredo, N.S.; Sampaio, L.S.; Magalhães, H.I.; Cavalcanti, B.C.; Gaspar, D.M.; de Andrade, G.M.; Lima, I.S.; et al. Synergistic effect of the flavonoids catechin, quercetin and epigallocatechin gallate with fluconazole induce apoptosis in *Candida tropicalis* resistant to fluconazole. *Antimicrob. Agents Chemother.* **2016**, *60*, 3551–3557. [[CrossRef](#)] [[PubMed](#)]
15. Kim, K.S.; Duncan, B.; Creran, B.; Rotello, V.M. Triggered Nanoparticles as Therapeutics. *Nano Today* **2013**, *8*, 439–447. [[CrossRef](#)] [[PubMed](#)]
16. Chrisey, D.B.; McGill, R.A.; Horwitz, J.S.; Pique, A.; Ringeisen, B.R.; Bubb, D.M.; Wu, P.K. Novel Laser-Based Deposition of Active Protein Thin Films. *Chem. Rev.* **2003**, *103*, 553–576. [[CrossRef](#)] [[PubMed](#)]
17. McGill, R.A.; Chrisey, D.B. Method of Producing a Film Coating by Matrix Assisted Pulsed Laser Deposition. U.S. Patent No. 6,025,036, 15 February 2000.
18. Cristescu, R.; Stamatina, I.; Mihaiescu, D.E.; Ghica, C.; Albulescu, M.; Mihaiescu, I.N.; Chrisey, D.B. Pulsed Laser Deposition of Biocompatible Polymers: A Comparative Study in Case of Pullulan. *Thin Solid Films* **2004**, *453–454*, 262–268. [[CrossRef](#)]
19. Cristescu, R.; Popescu, C.; Popescu, A.; Grigorescu, S.; Duta, L.; Caraene, G.; Ionescu, A.; Mihaiescu, D.; Albulescu, R.; Buruiana, T.; et al. Functionalized polyvinyl alcohol derivatives thin films for controlled drug release and targeting systems: MAPLE deposition and morphological, chemical and in vitro characterization. *Appl. Surf. Sci.* **2009**, *255*, 5600–5604. [[CrossRef](#)]
20. Cristescu, R.; Popescu, C.; Socol, G.; Iordache, I.; Mihaiescu, I.N.; Mihaiescu, D.E.; Grumezescu, A.M.; Balan, A.; Stamatina, I.; Chifiriuc, C.; et al. Magnetic core/shell nanoparticle thin films deposited by MAPLE: Investigation by chemical, morphological and in vitro biological assays. *Appl. Surf. Sci.* **2012**, *258*, 9250–9255. [[CrossRef](#)]
21. Cristescu, R.; Popescu, C.; Popescu, A.C.; Socol, G.; Mihaiescu, I.; Caraene, G.; Albulescu, R.; Buruiana, T.; Chrisey, D. Pulsed Laser Processing of Functionalized Polysaccharides for Controlled Release Drug Delivery Systems. In *Technological Innovations in Sensing and Detection of Chemical, Biological, Radiological, Nuclear Threats and Ecological Terrorism*; Vaseashta, A., Braman, E., Susmann, P., Eds.; NATO Science for Peace and Security Series A: Chemistry and Biology Book Series; Springer: Dordrecht, The Netherlands, 2012; Part 4; pp. 231–236. ISBN 978-94-007-2488-4.
22. Ge, W.; Yu, Q.; Lopez, G.P.; Stiff-Roberts, A.D. Antimicrobial oligo(p-phenylene-ethynylene) film deposited by resonant infrared matrix-assisted pulsed laser evaporation. *Colloids Surf. B Biointerfaces* **2014**, *116*, 786–792. [[CrossRef](#)]
23. Yu, Q.; Ge, W.; Atewologun, A.; Stiff-Roberts, A.D.; Lopez, G.P. Antimicrobial and bacteria-releasing multifunctional surfaces: Oligo (p-phenylene-ethynylene)/poly (N-isopropylacrylamide) films deposited by RIR-MAPLE. *Colloids Surf. B Biointerfaces* **2015**, *126*, 328–334. [[CrossRef](#)]
24. Cristescu, R.; Popescu, C.; Socol, G.; Visan, A.; Mihaiescu, I.N.; Gittard, S.D.; Miller, P.R.; Martin, T.N.; Narayan, R.J.; Andronie, A.; et al. Deposition of antibacterial of poly(1,3-bis-(p-carboxyphenoxy propane)-co-(sebacic anhydride)) 20:80/gentamicin sulfate composite coatings by MAPLE. *Appl. Surf. Sci.* **2011**, *257*, 5287–5292. [[CrossRef](#)]
25. Cristescu, R.; Dorcioman, G.; Miroiu, F.M.; Socol, G.; Mihaiescu, I.N.; Gittard, S.D.; Miller, P.R.; Narayan, R.J.; Enculescu, M.; Chrisey, D.B. Antimicrobial activity of biopolymer–antibiotic thin films fabricated by advanced pulsed laser methods. *Appl. Surf. Sci.* **2013**, *278*, 211–213. [[CrossRef](#)]

26. Cristescu, R.; Visan, A.; Socol, G.; Surdu, A.V.; Oprea, A.E.; Grumezescu, A.M.; Chifiriuc, M.C.; Boehm, R.D.; Yamaleyeva, D.; Taylor, M.; et al. Antimicrobial activity of biopolymeric thin films containing flavonoid natural compounds and silver nanoparticles fabricated by MAPLE: A comparative study. *Appl. Surf. Sci.* **2016**, *374*, 290–296. [[CrossRef](#)]
27. Cristescu, R.; Surdu, A.V.; Grumezescu, A.M.; Oprea, A.E.; Trusca, R.; Vasile, O.; Dorcioman, G.; Visan, A.; Socol, G.; Mihailescu, I.N.; et al. Microbial Colonization of Biopolymeric Thin Films Containing Natural Compounds and Antibiotics Fabricated by MAPLE. *Appl. Surf. Sci.* **2015**, *336*, 234–239. [[CrossRef](#)]
28. Binns, C. *Introduction to Nanoscience and Nanotechnology*; John Wiley & Sons Inc.: Hoboken, NJ, USA, 2010.
29. Mortale, S.P.; Karuppayil, S.M. Review on Combinatorial Approach for Inhibiting *Candida albicans* Biofilm. *Am. J. Clin. Microbiol. Antimicrob.* **2018**, *1*, 1022.
30. Andrew, S.; Hitchcock, C.A.; Dorr, P.K. Antifungal Compositions Comprising Voriconazole and Trovafloxacin or Prodrugs Thereof. Patent EP0982031A2, 1 March 2000.
31. Sun, L.; Liao, K.; Li, Y.; Zhao, L.; Liang, S.; Guo, D.; Hu, J.; Wang, D. Synergy Between Polyvinylpyrrolidone-Coated Silver Nanoparticles and Azole Antifungal Against Drug-Resistant *Candida albicans*. *J. Nanosci. Nanotechnol.* **2016**, *16*, 2325–2335. [[CrossRef](#)] [[PubMed](#)]



© 2019 by the authors. Licensee MDPI, Basel, Switzerland. This article is an open access article distributed under the terms and conditions of the Creative Commons Attribution (CC BY) license (<http://creativecommons.org/licenses/by/4.0/>).